X-rays from the Highly Polarized Broad Absorption Line QSO CSO 755

W. N. Brandt,[1] A. Comastri,[2] S. C. Gallagher,[1] R. M. Sambruna,[1] Th. Boller[3] and A. Laor[4]

ABSTRACT

We present results from a *BeppoSAX* observation of the BAL QSO CSO 755, observed as part of our program to investigate the X-ray properties of highly polarized BAL QSOs. CSO 755 is clearly detected by the *BeppoSAX* MECS, making it the highest redshift ($z = 2.88$) and most optically luminous ($M_{\rm V} = -27.4$) BAL QSO seen in X-rays. It is detected in several energy bands including the rest-frame 21–39 keV band, but we are only able to place loose constraints upon its X-ray spectral shape. Our X-ray detection is consistent with the hypothesis that the BAL QSOs with high optical continuum polarization tend to be the X-ray brighter members of the class. We examine a scattering interpretation of a polarization/X-ray flux connection, and we discuss the data needed to prove or refute such a connection. We also discuss a probable *ROSAT* detection of CSO 755. The observed-frame 2–10 keV flux from *BeppoSAX* (1.3×10^{-13} erg cm^{-2} s^{-1}) is high enough to allow *XMM* spectroscopy, and studies of iron K line emission should prove of particular interest if a large amount of scattered X-ray flux is present.

Subject headings: quasars: individual (CSO 755) – galaxies: active – galaxies: nuclei – quasars: general – X-rays: galaxies.

1. Introduction

The ejection of matter at moderate to high velocities is a common and perhaps universal phenomenon of Quasi-Stellar Objects (QSOs). One of the main manifestations

---

[1]Department of Astronomy and Astrophysics, 525 Davey Laboratory, Pennsylvania State University, University Park, PA 16802

[2]Osservatorio Astronomico di Bologna, via Ranzani 1, I-40127 Bologna, Italy

[3]Max-Planck-Institut für Extraterrestrische Physik, 85748 Garching, Germany

[4]Physics Department, Technion, Haifa 32000, Israel

of QSO outflows is the blueshifted UV Broad Absorption Lines (BALs) seen in $\sim 10\%$ of optically selected QSOs, the BAL QSOs (e.g., Weymann 1997). X-ray spectroscopy of BAL QSOs is potentially important for studying their outflows and nuclear geometries, but the study of BAL QSOs in the X-ray regime has not yet matured, largely due to low X-ray fluxes (e.g., Green & Mathur 1996; Gallagher et al. 1999). Only ≈ 9 BAL QSOs have been detected in X-rays at present. The current data suggest that the X-ray emission from BAL QSOs suffers from significant intrinsic absorption, with many BAL QSOs having absorption column densities $\gtrsim$ (1–5)$\times 10^{23}$ cm^{-2}. Optical brightness is *not* a good predictor of X-ray brightness for BALQSOs; some optically faint BAL QSOs have been clearly detected (e.g., PHL 5200; $V = 18.1$) while some of the optically brightest (e.g., PG $1700+518$; $V = 15.1$) remain undetected in deep 0.1–10 keV observations. In the limited data available at present, however, there is a suggestion that the BAL QSOs with high ($\gtrsim 2\%$) optical continuum polarization *may* be the X-ray brighter members of the class (see §4 of Gallagher et al. 1999). A polarization/X-ray flux connection, if indeed present, would provide a clue about the geometry of matter in BAL QSO nuclei (see §3).

To improve understanding of the X-ray properties of BAL QSOs and examine the possible polarization/X-ray flux connection, we have started a program to observe highly polarized BAL QSOs in X-rays. An excellent target for this program was the Case Stellar Object 755 (CSO 755; $z = 2.88$; Sanduleak & Pesch 1989), which has $V = 17.1$ (e.g., Barlow 1993) and is a representative, 'bona-fide' BAL QSO in terms of its luminosity and UV absorption properties (e.g., Glenn et al. 1994). Its continuum polarization is high (≈ 3.8–4.7%; only 8/53 BAL QSOs studied by Schmidt & Hines 1999 had $> 2\%$) and rises to the blue.

We adopt $H_0 = 70$ km s^{-1} Mpc^{-1} and $q_0 = \frac{1}{2}$. The Galactic neutral hydrogen column density towards CSO 755 is $(1.6 \pm 0.4) \times 10^{20}$ cm^{-2} (Stark et al. 1992).

2. Observations, Analysis and Results

We observed CSO 755 with *BeppoSAX* (Boella et al. 1997) on 1999 Feb 2. We will focus on the results from the Medium-Energy Concentrator Spectrometers (MECS; 1.8–10 keV; 35.2 ks exposure) and Low-Energy Concentrator Spectrometer (LECS; 0.1–4 keV; 12.7 ks exposure), since the data from the other instruments are not useful for such a faint source. Our energy coverage corresponds to 0.4–39 keV in the rest frame. The observation went smoothly, and the resulting data were processed with Version 1.2 of the *BeppoSAX* Science Data Center (BSDC) pipeline. We have adopted the standard reduction methods recommended by the BSDC (Fiore, Guainazzi & Grandi 1999), and we do not observe any irregular background variability.

The screened events resulting from the above reduction were analyzed using XSELECT. We made full-band images for each of the detectors as well as combined MECS2+MECS3 images. An X-ray source consistent with the precise optical position of CSO 755 is detected with high statistical significance in our MECS2, MECS3 and MECS2+MECS3 images (e.g., Figure 1), but it is not detected by the LECS. Given the observed flux (see below), the probability of a confusing source is $\lesssim 5 \times 10^{-3}$, and no particularly suspicious sources are found in the Palomar Optical Sky Survey or the NED/SIMBAD catalogs. To determine MECS count rates, we have used a $3'$-radius circular source cell centered on the X-ray centroid. For background subtraction, we use five $3'$-radius circular cells near CSO 755 (we have not used an annulus because a weak nearby source would fall inside the annulus). We have corrected for energy-dependent vignetting of the background following §3.1.5 of Fiore et al. (1999). In the MECS2+MECS3 full-band (1.8–10 keV) image, we detect 54.3 ± 14.3 counts from CSO 755 for a MECS2+MECS3 count rate of $(1.5 \pm 0.4) \times 10^{-3}$ count s^{-1}. The LECS 3σ upper limit on the 0.1–1.8 keV count rate is $< 1.7 \times 10^{-3}$ count s^{-1} (computed using a circular source cell with a $5'$ radius).

While we do not have enough photons for spectral fitting, we have analyzed MECS2+MECS3 images in three observed-frame energy bands to place crude constraints on spectral shape: 1.8–3 keV (band 1; channels 40–66), 3–5.5 keV (band 2; channels 67–120), and 5.5–10 keV (band 3; channels 121–218). CSO 755 is detected in all bands, although with varying degrees of statistical significance. We give the corresponding count rates in Table 1, and the Poisson probabilities of false detections in bands 1, 2 and 3 are 6.8×10^{-5}, 4.8×10^{-3} and 2.8×10^{-2}, respectively. The detection in band 3 (21–39 keV in the rest frame) is notable.

To compare the observed spectral shape with spectral models, we have employed a band-fraction diagram similar to those used in studies of the diffuse soft X-ray background (e.g., see §5 of Burstein et al. 1977). We first consider a simple power-law model with photon index, $\Gamma = 1.7$–1.9 (a typical, representative range for radio-quiet QSOs; e.g. Reeves et al. 1997), and neutral absorption at $z = 2.88$. For this model, Figure 2 shows that column densities less than $\approx 7 \times 10^{23}$ cm^{-2} are most consistent with our data. Alternatively, for small column densities, values of Γ down to ≈ 0.8 are most consistent with our data (i.e. the spectrum could be as flat as that for a 'reflection-dominated' source). Incorporating the LECS upper limit into similar analyses does not significantly tighten our constraints.

If we consider a $\Gamma = 1.9$ power-law model with the Galactic column density, we calculate an observed-frame 2–10 keV flux of 1.3×10^{-13} erg cm^{-2} s^{-1}, corresponding to a rest-frame 7.8–39 keV luminosity of 4.0×10^{45} erg s^{-1}. These two quantities are relatively insensitive to the internal column density for $N_{\rm H} < 5 \times 10^{23}$ cm^{-2}. If we extrapolate this model into the rest-frame 2–10 keV band, the luminosity is 3.4×10^{45} erg s^{-1}.

We have also calculated $\alpha_{\rm ox}$ (the slope of a hypothetical power law between 3000 Å and 2 keV in the rest frame), since this parameter can be used as a statistical predictor of the presence of X-ray absorption (e.g., Brandt, Laor & Wills 1999). We calculate the rest-frame 3000 Å flux density using the observed-frame 7500 Å flux density of Glenn et al. (1994) and a continuum spectral index of $\alpha = 0.5$. The rest-frame flux density at 2 keV is more difficult to calculate since we do not have strong constraints on X-ray spectral shape or a *BeppoSAX* detection at $\frac{2\ {\rm keV}}{(1+z)} = 0.52$ keV (although see our discussion of the *ROSAT* data below). If we normalize a $\Gamma = 1.9$ power-law model with Galactic absorption to the rest frame 7–39 keV count rate (corresponding to 1.8–10 keV in the observed frame), we calculate $\alpha_{\rm ox} = 1.58$. Of course, this $\alpha_{\rm ox}$ value is really telling us about the rest-frame 7–39 keV emission rather than a directly measured flux density at 2 keV.

We have searched for any *Einstein*, *ROSAT* or *ASCA* pointings that serendipitously contain CSO 755, but unfortunately there is none. We have also analyzed the data from the *ROSAT* All-Sky Survey (RASS). CSO 755 was observed for 939 s during the RASS between 1990 Dec 31 and 1991 Jan 4 (a relatively long RASS exposure; see Figure 2 of Voges et al. 1999). There appears to be an ≈ 7-photon enhancement over the average background at the position of CSO 755. Comparative studies of RASS and pointed data show that $\approx 90\%$ of such 7-photon RASS sources are real X-ray sources rather than statistical fluctuations, and CSO 755 is included in the Max-Planck-Institut für Extraterrestrische Physik RASS faint source catalog (Voges et al., in preparation) with a likelihood of 11 (see Cruddace, Hasinger & Schmitt 1988). However, to be appropriately cautious we shall treat the probable RASS detection as tentative. The probable RASS detection corresponds to a vignetting-corrected flux in the observed 0.1–2.4 keV band of $\approx\ 1.1 \times 10^{-13}$ erg cm^{-2} s^{-1} (for a power-law model with $\Gamma = 1.9$ and the Galactic absorption column). Given the relative effective areas and imaging capabilities of the *ROSAT* PSPC and *BeppoSAX* LECS, a RASS detection is consistent with the LECS upper limit given in Table 1 (see Figure 2 of Parmar et al. 1999). Provided there is not substantial intrinsic X-ray absorption below the MECS band, the relative RASS and MECS fluxes are entirely plausible. If we use the *ROSAT* flux to normalize a $\Gamma = 1.9$ power law with Galactic absorption, we calculate $\alpha_{\rm ox} = 1.62$. If *ROSAT* has indeed detected CSO 755, the *ROSAT* band has the advantage that it directly constrains the rest-frame 2 keV flux density.

3. Discussion and Conclusions

Our *BeppoSAX* and probable *ROSAT* detections of CSO 755 make it the highest redshift as well as the most optically luminous BAL QSO detected in X-rays. It was selected for study not based upon high optical flux but rather based on its high (observed-frame) optical continuum polarization (3.8–4.7%; hereafter OCP), and it is X-ray brighter than several other BAL QSOs that have $\approx$ 4–6 times its V-band flux (compare with Gallagher et al. 1999). While its higher X-ray flux could partially result from the higher redshift providing access to more penetrating X-rays (i.e. a 'negative K-correction'), there is also suggestive evidence that the BAL QSOs with high OCP may be the X-ray brighter members of the class.

We have investigated the OCP percentages of the 10 BAL QSOs (including CSO 755) with reliable X-ray detections using the data from Berriman et al. (1990), Hutsemékers, Lamy & Remy (1998), Ogle (1998) and Schmidt & Hines (1999). The OCP percentages have a mean of 2.28 ± 0.28, a standard deviation of 0.88, and a median of 2.24. These values indeed place the X-ray detected BAL QSOs toward the high end of the BAL QSO OCP distribution function (compare with §2 of Schmidt & Hines 1999). At present, however, our nonparametric testing is unable to prove that the X-ray detected BAL QSOs have higher OCPs than those that are undetected in sensitive X-ray observations. This is due to small sample sizes as well as concerns about possible secondary correlations and observational biases. Many of the BAL QSOs with high-quality X-ray data have been observed because they have exceptional properties (e.g., low-ionization absorption, extreme Fe II emission), and thus the currently available sample is not necessarily representative of the population as a whole. In addition, the current X-ray and polarization observations of BAL QSOs span a wide range of rest-frame energy/wavelength bands due to redshift and instrumentation differences (redshifts for the 10 X-ray detected BAL QSOs run from z = 0.042–2.88). At higher redshifts one samples harder X-rays that are less susceptible to absorption. Also at higher redshifts, observed-frame OCP measurements tend to sample shorter wavelengths, and many QSOs show polarization that rises towards the blue. Systematic X-ray and polarimetric observations of uniform, well-defined BAL QSO samples are needed to examine this issue better.

A polarization/X-ray flux connection could be physically understood if the direct lines of sight into the X-ray nuclei of BAL QSOs were usually blocked by extremely thick matter ($\gg 10^{24}$ cm^{-2}). In this case, we could only see X-rays when there is a substantial amount of electron scattering in the nuclear environment by a 'mirror' of moderate Thomson depth.[5]

[5] Ogle (1998) suggests that there is a large range of mirror optical depths among the BAL QSO population.

The scattering would provide a periscopic, indirect view into the compact X-ray emitting region while also polarizing some of the more extended optical continuum emission (see Figure 3). Measured X-ray column densities would then provide information only about the gas along the *indirect* line of sight. For CSO 755, the X-ray scattering medium would need to be located on fairly small scales ($\lesssim$ a few light weeks) to satisfy the spectropolarimetric constraints of Glenn et al. (1994) and Ogle (1998). These show that the material scattering the optical light is located at smaller radii than both the Broad Line Region (BLR) and BAL region.

Our calculations in §2 give an $\alpha_{\rm ox}$ value of ≈ 1.6, although our only direct constraint on the rest-frame 2 keV flux density is via the probable *ROSAT* detection. Our $\alpha_{\rm ox}$ value is entirely consistent with those of typical radio-quiet QSOs (compare with Figure 1 of Brandt, Laor & Wills 1999), and it is smaller than those of many BAL QSOs (e.g. Green & Mathur 1996). A 'normal' $\alpha_{\rm ox}$ value would appear somewhat surprising in the context of the scattering model of the previous paragraph, since one would expect the X-ray flux level to be reduced if the direct line of sight is blocked. However, there is enough dispersion in the $\alpha_{\rm ox}$ distribution that the observed value of $\alpha_{\rm ox}$ does not cause a serious problem, provided the scattering is efficient. The scattering mirror would need to subtend a fairly large solid angle (as seen by the compact X-ray source) and have a moderate Thomson depth (say $\tau_{\rm T} \sim 0.3$). In addition, there may be 'attenuation' at 3000 Å (in the sense of §2 of Goodrich 1997) that helps to flatten $\alpha_{\rm ox}$.

Finally, we note that CSO 755 has a high enough X-ray flux to allow moderate quality X-ray spectroscopy and variability studies with *XMM*. It is currently scheduled for a 5 ks *XMM* observation, but this is an inadequate exposure time for such work. A longer *XMM* exposure would allow a study of any iron K spectral features, and the high redshift of CSO 755 moves the iron K complex right to the peak of the *XMM* EPIC spectral response. If we are viewing a large amount of scattered X-ray flux in CSO 755 and other high polarization BAL QSOs, then narrow iron K lines with large equivalent widths may be produced via fluorescence and resonant scattering (as for the much less luminous Seyfert 2 galaxies; e.g., Krolik & Kallman 1987). Such lines could allow direct detection of the X-ray scattering medium, and line energies and blueshifts/redshifts would constrain the ionization state and dynamics of the mirror. We would also not expect rapid ($\lesssim$ 1 day) and large-amplitude X-ray variability if most of the X-ray flux is scattered.

We thank J. Halpern, J. Nousek, W. Voges and B. Wills for helpful discussions, and we thank H. Ebeling for the use of his IDL software. We acknowledge the support of NASA LTSA grant NAG5-8107 (WNB), Italian Space Agency contract ASI-ARS-98-119 and MURST grant Cofin-98-02-32 (AC), NASA grant NAG5-4826 and the Pennsylvania Space

Grant Consortium (SCG), and the fund for the promotion of research at the Technion (AL).

REFERENCES

Barlow, T. A. 1993, PhD thesis, UC San Diego

Boella, G., Butler, R. C., Perola, G. C., Piro, L., Scarsi, L. & Bleeker, J. 1997, A&AS, 122, 299

Brandt, W. N., Laor, A. & Wills, B. J. 1999, ApJ, in press (astro-ph/9908016)

Berriman, G., Schmidt, G. D., West, S. C. & Stockman, H. S. 1990, ApJS, 74, 869

Burstein, P., Borken, R. J., Kraushaar W. L. & Sander, W. T. 1977, ApJ, 213, 405

Cruddace, R. G., Hasinger, G. R. & Schmitt, J. H. M. M. 1988, in Astronomy from Large Databases: Scientific Objectives and Methodological Approaches, ed. Murtagh, F. & Heck, A. (ESO Press, Garching), p. 177

Ebeling, H., White, D. A. & Rangarajan, F. V. N. 1999, MNRAS, in press

Fiore, F., Guainazzi, M. & Grandi, P. 1999, Cookbook for NFI Scientific Data Analysis. *BeppoSAX* Science Data Center, Rome

Gallagher, S. C., Brandt, W. N., Sambruna, R. M., Mathur, S. & Yamasaki, N. 1999, ApJ, 519, 549

Glenn, J., Schmidt, G. D. & Foltz, C. B. 1994, ApJ, 434, L47

Goodrich, R. W. 1997, ApJ, 474, 606

Green, P. J. & Mathur, S. 1996, ApJ, 462, 637

Hutsemékers, D., Lamy, H. & Remy, M. 1998, A&A, 340, 371

Krolik, J. H. & Kallman, T. R. 1987, ApJ, 320, L5

Lyons, L. 1991, Data Analysis for Physical Science Students, Cambridge University Press, Cambridge

Ogle, P. M. 1998, PhD thesis, California Institute of Technology

Parmar, A. et al. 1999, A&A, in press (astro-ph/9902075)

Reeves, J. N., Turner, M. J. L., Ohashi, T. & Kii, T. 1997, MNRAS, 292, 468

Sanduleak, N. & Pesch, P. 1989, ApJS, 70, 173

Schmidt, G. D. & Hines, D. C. 1999, ApJ, 512, 125

Stark, A. A., Gammie, C. F., Wilson, R. W., Bally, J., Linke, R.A., Heiles, C. & Hurwitz, M. 1992, ApJS, 79, 77

Voges, W. et al. 1999, A&A, in press

Weymann, R. J. 1997, in Mass Ejection from AGN, ed. Arav, N., Shlosman, I. & Weymann, R. J. (ASP Press: San Francisco), p. 3

This preprint was prepared with the AAS LATEX macros v4.0.

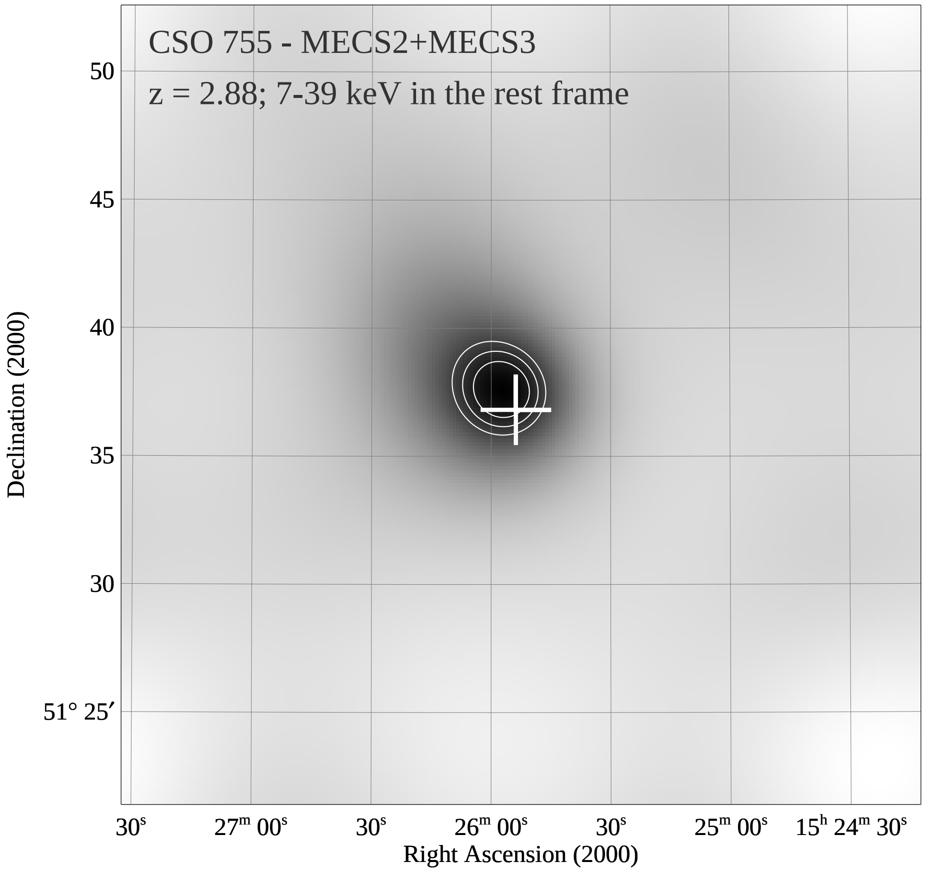

Fig. 1.— MECS2+MECS3 image of CSO 755 made using the full-band (1.8–10 keV) data. This energy range corresponds to 7–39 keV in the rest frame. The image has been adaptively smoothed using the algorithm of Ebeling, White & Rangarajan (1999). The contours are drawn at 85.1, 89.4 and 93.7% of the maximum pixel value, and the white cross marks the precise optical position of CSO 755.

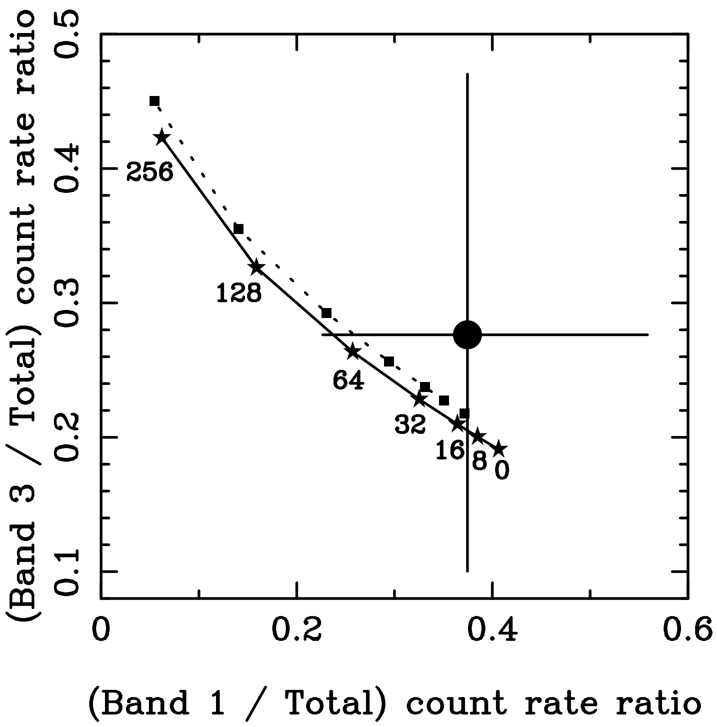

Fig. 2.— Band-fraction diagram for CSO 755. The large solid dot with error bars shows the position of CSO 755. The error bars have been computed using the 'numerical method' described in §1.7.3 of Lyons (1991) and roughly correspond to 1σ. The stars and solid curve show the locus of a power-law model with photon index $\Gamma = 1.9$ and varying amounts of $z = 2.88$ neutral absorption ($N_{\rm H}$). The squares and dotted curve show the same for a power-law model with $\Gamma = 1.7$. Absorption increases towards the left, and the individual symbols along each curve correspond to $N_{\rm H}$ values of (0, 8, 16, 32, 64, 128 and 256)$\times 10^{22}$ cm^{-2}. The stars for the $\Gamma = 1.9$ case have been labeled in units of 10^{22} cm^{-2}.

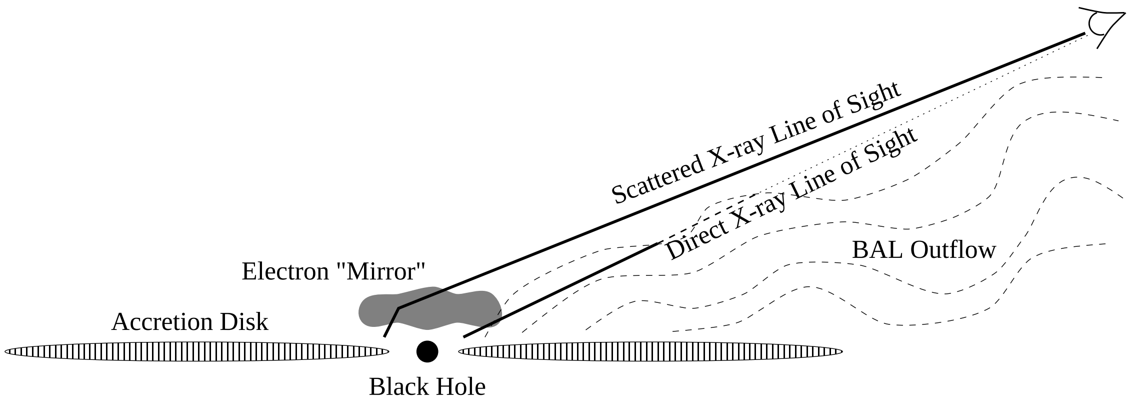

Fig. 3.— A schematic model showing the possible X-ray lines of sight in a highly polarized BAL QSO. X-rays which would travel directly to the observer are strongly absorbed by extremely thick matter ($\gg 10^{24}$ cm^{-2}). X-rays that are scattered by a compact electron 'mirror' of moderate Thomson depth are able to reach the observer with significantly less absorption and thus dominate the observed flux. While we have drawn the BAL outflow to be the X-ray absorbing matter, we note that this has not been demonstrated to be the case.

TABLE 1

Count Rates in the Observed Frame

Instrument & Energy Band	Count Rate / (10^{-4} Count s^{-1})
BeppoSAX LECS	
0.1–1.8 keV	< 17
BeppoSAX MECS2+MECS3	
1.8–3 keV (band 1)	5.8 ± 1.9
3–5.5 keV (band 2)	5.4 ± 2.5
5.5–10 keV (band 3)	4.3 ± 2.6
1.8–10 keV (full band)	15 ± 4

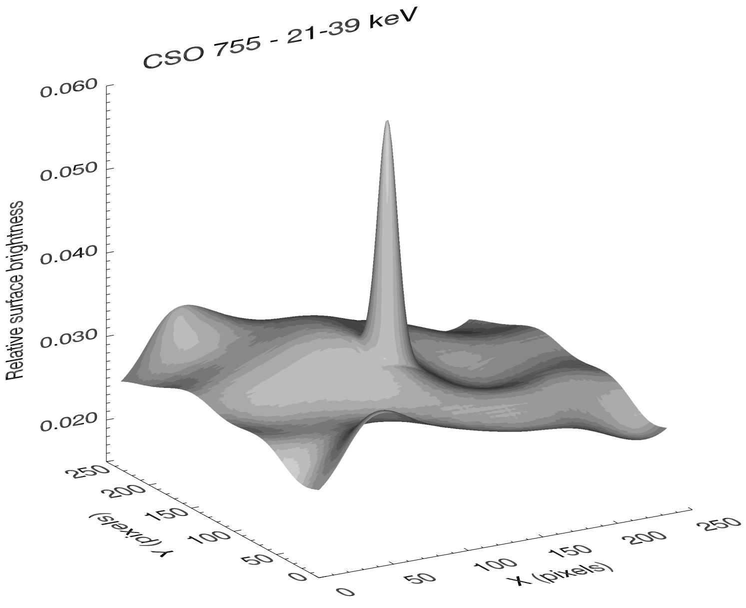

Fig. 4.— Three-dimensional representation of the 5.5–10 keV (band 3) image from MECS2+MECS3. The image has been adaptively smoothed, and it corresponds to 21–39 keV in the rest frame. The peak in the center of the image is CSO 755. This is an unofficial 'bonus' figure that will not appear in the ApJL publication.